NATIONAL ADVISORY COMMITTEE
FOR AERONAUTICS

TECHNICAL NOTE 3569

COMPRESSIBLE LAMINAR BOUNDARY LAYER AND HEAT TRANSFER

FOR UNSTEADY MOTIONS OF A FLAT PLATE

By Simon Ostrach

Lewis Flight Propulsion Laboratory
Cleveland, Ohio

NACA

Washington

November 1955

NATIONAL ADVISORY COMMITTEE FOR AERONAUTICS

TECHNICAL NOTE 3569

COMPRESSIBLE LAMINAR BOUNDARY LAYER AND HEAT TRANSFER

FOR UNSTEADY MOTIONS OF A FLAT PLATE

By Simon Ostrach

SUMMARY

The laminar compressible boundary layer and heat transfer over an isothermal semi-infinite flat plate moving with a time-dependent velocity has been analyzed. First-order deviations from the quasi-steady velocity and temperature profiles and boundary-layer characteristics have been computed. For a plate oscillating about a steady velocity, it is shown that the maxima of skin-friction coefficient and local heat-transfer rate are out of phase with the plate velocity; the skin friction leads by angles not exceeding $45°$ for permissible values of the frequency parameter, whereas the heat transfer is almost in phase with the plate velocity for very small Mach numbers but depends significantly on the Mach number, plate to stream temperature ratio, and frequency for higher-speed flows.

INTRODUCTION

Until recently, studies of unsteady laminar boundary layer were limited either to the early stages of the motion (i.e., to the transient state) or to oscillatory motions without a mean flow. The fluid, furthermore, was assumed to be incompressible. More detailed investigations were not made, because it was felt that the boundary-layer growth occurred in so short a period of time that, for engineering purposes, the flow could be assumed steady. However, in many present-day applications, consideration must be given to the unsteady effects for long periods of time and for high-speed flows in which compressibility is important. For example, the skin friction and heat transfer of the usual rocket missile must be regarded as unsteady for its entire flight because the flight speed varies continuously over the entire trajectory. Other cases of importance in this regard include blades rotating in non-uniform air streams, unsteady nozzle flow, and oscillating wings.

Accordingly, the unsteady laminar compressible boundary layer over an insulated surface was analyzed in reference 1. The development therein is for continuous time-dependent velocities of the body, and universal functions are presented from which the deviations of the velocity and temperature profiles from the quasi-steady state[1] can be determined.

To determine the effects of free-stream fluctuations on both skin friction and heat transfer, the case of two-dimensional incompressible flow about a fixed cylindrical body is treated in reference 2 by an integral method.

In the present paper, prepared at the NACA Lewis laboratory, consideration is given to the laminar compressible boundary layer and heat transfer over a semi-infinite flat plate maintained at a uniform (both temporally and spatially) temperature and moving with a continuous but otherwise arbitrary time-dependent velocity. The solutions are obtained as a series about the quasi-steady state. The analysis presented herein, therefore, extends the results of reference 1 to include the effects of heat transfer. The present study also represents a more exact treatment including compressibility effects of a similar[2] problem treated in reference 2.

ANALYSIS

Basic Equations

Consideration is given herein to the laminar flow and heat transfer about an isothermal semi-infinite flat plate in rectilinear flight through still air; the flight speed is to be time-dependent. For this flow it is presumed that the Prandtl boundary-layer assumptions are valid, and, in particular, the pressure is constant throughout the fluid. If it is further assumed that the Prandtl number and specific

---

[1]When the boundary layer at any instant is that appropriate to steady flow at the instantaneous value of the stream velocity, the flow is said to be quasi steady.

[2]The class of bodies considered in reference 2 is more general than that considered herein.

heat are constant, the equations governing the flow and heat transfer
in a compressible viscous fluid are

$$\frac{\partial \rho}{\partial t} + \frac{\partial}{\partial x} (\rho \bar{u}) + \frac{\partial}{\partial y} (\rho \bar{v}) = 0$$

$$\rho\left(\frac{\partial \bar{u}}{\partial t} + \bar{u} \frac{\partial \bar{u}}{\partial x} + \bar{v} \frac{\partial \bar{u}}{\partial y}\right) = \frac{\partial}{\partial y}\left(\mu \frac{\partial \bar{u}}{\partial y}\right)$$

$$\rho\left(\frac{\partial \theta}{\partial t} + \bar{u} \frac{\partial \theta}{\partial x} + \bar{v} \frac{\partial \theta}{\partial y}\right) = \frac{1}{Pr} \frac{\partial}{\partial y}\left(\mu \frac{\partial \theta}{\partial y}\right) + \frac{\mu}{c_p}\left(\frac{\partial \bar{u}}{\partial y}\right)^2$$

$$\rho\theta = \text{const}$$

(1)

where the symbols are defined in appendix A.

These equations are written for a rectangular coordinate system
which is stationary in the fluid. The plate, therefore, moves with a
velocity $U(\bar{t})$ in the negative $\bar{x}$-direction, and $\bar{y}$ is measured normal
to the plate (see fig. 1(a)). The origin of coordinates is taken to
be the leading-edge location at $\bar{t} = 0$.

These equations may be written in another coordinate system fixed
with reference to the plate, with the origin at the leading edge (see
fig. 1(b)). The appropriate transformations for this change of coordi-
nates are

$$u \equiv \bar{u} + U; \qquad v \equiv \bar{v}$$

$$x \equiv \bar{x} + \int_0^{\bar{t}} U \, d\bar{t}; \qquad y \equiv \bar{y}; \qquad t \equiv \bar{t}$$

Equation (1) then becomes

$$\frac{\partial \rho}{\partial t} + \frac{\partial}{\partial x} (\rho u) + \frac{\partial}{\partial y} (\rho v) = 0$$

$$\rho\left(\frac{\partial u}{\partial t} + u \frac{\partial u}{\partial x} + v \frac{\partial u}{\partial y}\right) = \rho \frac{dU}{dt} + \frac{\partial}{\partial y}\left(\mu \frac{\partial u}{\partial y}\right)$$

$$\rho\left(\frac{\partial \theta}{\partial t} + u \frac{\partial \theta}{\partial x} + v \frac{\partial \theta}{\partial y}\right) = \frac{1}{Pr} \frac{\partial}{\partial y}\left(\mu \frac{\partial \theta}{\partial y}\right) + \frac{\mu}{c_p}\left(\frac{\partial u}{\partial y}\right)^2$$

$$\rho\theta = \text{const}$$

(2)

The variation of viscosity with temperature is approximated by

$$\mu = \mu_\infty C \frac{\theta}{\theta_\infty} = \rho_\infty \nu_\infty C \frac{\theta}{\theta_\infty} \tag{3}$$

as is discussed in reference 3. The constant C is obtained by matching equation (3) with the Sutherland formula at some appropriate point. If the matching is done at the wall,

$$C = \sqrt{\frac{\theta_W}{\theta_\infty}} \left(\frac{\theta_\infty + 216^\circ \text{ R}}{\theta_W + 216^\circ \text{ R}} \right) \tag{4}$$

The momentum equation can be made independent of the energy equation by means of the transformation

$$Y \equiv \int_0^y \frac{\rho}{\rho_\infty} \, dy; \quad X \equiv x; \quad T \equiv t \tag{5}$$

which is similar to that used in reference 4. Further simplification of the basic equations will result from the introduction of a stream function as in reference 1:

$$\left. \begin{aligned} u &\equiv \frac{\rho_\infty}{\rho} \frac{\partial \psi}{\partial y} = \frac{\partial \psi}{\partial Y} \\[2ex] v &\equiv -\frac{\rho_\infty}{\rho} \left(\frac{\partial \psi}{\partial x} + \frac{\partial}{\partial t} \int_0^y \frac{\rho}{\rho_\infty} \, dy \right) = -\frac{\rho_\infty}{\rho} \left(\frac{\partial \psi}{\partial X} + \frac{\partial \psi}{\partial Y} \frac{\partial Y}{\partial x} + \frac{\partial Y}{\partial t} \right) \end{aligned} \right\} \tag{6}$$

and the definition

$$\Theta = \frac{\theta - \theta_\infty}{\theta_W - \theta_\infty} \tag{7}$$

Application of equations (4) to (7) to equations (2) yields

$$\psi_{YT} + \psi_Y \psi_{XY} - \psi_X \psi_{YY} = U'(T) + C\nu_\infty \psi_{YYY} \tag{8a}$$

$$\Theta_T + \psi_Y \Theta_X - \psi_X \Theta_Y = \frac{C\nu_\infty}{\text{Pr}} \Theta_{YY} + \frac{C\nu_\infty}{c_p(\theta_W - \theta_\infty)} (\psi_{YY})^2 \tag{8b}$$

The appropriate boundary conditions on ψ are

$$\psi_Y(X,\infty,T) = \psi_Y(0,Y,T) = U(T) \tag{9a}$$

$$\psi_Y(X,0,T) = \psi(X,0,T) = 0 \tag{9b}$$

For the case of an isothermal surface as considered herein, the boundary conditions on Θ are

$$\Theta(X,\infty,T) = \Theta(0,Y,T) = 0 \tag{10a}$$

$$\Theta(X,0,T) = 1 \tag{10b}$$

It should be noted that initial conditions would have to be added to these boundary conditions if the early stages of the motion are to be described properly. However, in the present problem it is assumed that sufficient time has elapsed so that the initial conditions no longer affect the flow.

Solutions

The solutions of the boundary-value problem (specified by eqs. (8) to (10)) describing the flow and heat transfer of an isothermal semi-infinite flat plate traveling in a compressible viscous medium with a speed that may vary with time in a differentiable but otherwise arbitrary manner will be obtained by a method similar to that of reference 1. That method is appropriately modified herein to include the effects of heat transfer.

Parameters. - It is desirable to determine the governing parameters before attempting to obtain a solution. Reference 1 noted that the dimensionless parameters

$$\frac{XU'}{U^2}; \quad \frac{X^2U''}{U^3}; \quad \ldots; \quad \frac{X^nU^{(n)}}{U^{n+1}}; \quad \ldots \tag{11}$$

can be formed from the coordinate along the surface and the stream velocity and its derivatives. The Reynolds and Mach numbers are, of course, also pertinent. Physically, the quantities (11) represent the ratio of the time required for a change of some physical quantity (e.g., velocity) at the boundary-layer edge to diffuse throughout the layer to the time that is characteristic of a variation of the free stream at the boundary-layer edge. Hence, the quantities (11) are a measure of the promptness with which the boundary layer responds to impressed changes. If the quantities (11) are very small, the flow can be considered to be quasi steady; that is, the boundary layer at any instant is that appropriate to steady flow at the instantaneous value of the stream velocity.

The significance of the parameters (11) can be made clearer, perhaps, by consideration of a special case. For uniform acceleration, for example, $U = AT$; and the quantities (11) reduce to a single parameter $\zeta = X/AT^2$, which is equivalent to the ratio of the distance aft of the leading edge to the distance traveled by the plate. For $\zeta \gg 1$, the effect of the leading edge has not yet been felt at the station X; and reference 1 points out that the solution for this condition corresponds to the initial motion. If $\zeta \ll 1$, the growth of the boundary layer with X must be considered; and reference 1 shows that for this case the flow is nearly quasi steady. Returning to the earlier interpretation of (11), it is clear that, if the velocity is increasing, the boundary layer at a fixed point on the plate becomes progressively thinner and, hence, responds more quickly to changes at its outer edges. This trend tends to establish quasi-steady flow.

Simplification for nearly quasi-steady flows. - In accord with reference 1, if consideration is restricted to a stage of motion where the flow is nearly quasi steady[3], the stream function may be defined as

$$\psi \equiv \sqrt{Cv_\infty UX} \; f(\sigma, \zeta_0, \zeta_1, \zeta_2, \cdot \cdot \cdot) \tag{12}$$

where $\sigma \equiv \dfrac{Y}{2} \sqrt{\dfrac{U}{Cv_\infty X}}$ and ζ_n are functions of X, T that characterize the departure from the quasi-steady state. The explicit definitions of the ζ_n are determined in the course of the analysis. The dimensionless temperature difference cannot be expressed in the usual manner (see ref. 3) in terms of two functions, one of which solves the thermometer (i.e., insulated plate) problem and the other corrects for the heat transfer, since the adiabatic wall temperature is a function of both X and T herein. Therefore, let

$$\Theta \equiv h(\sigma, \zeta_n) + \frac{U^2(T)}{2c_p(\theta_w - \theta_\infty)} \; s(\sigma, \zeta_n) \tag{13}$$

---

[3]The motion in the early stages, that is, before the flow becomes quasi steady, is treated for several configurations in reference 5. For this case, the inertia terms and the x-dependence vanish.

Substitution of equations (12) and (13) into equations (8) yields

$$f_{\sigma\sigma\sigma} + ff_{\sigma\sigma} = -8\frac{XU'}{U^2} + 2\left(2\frac{XU'}{U^2} + X\sum_{n=0}^{\infty}f_{\sigma\zeta_n}\zeta_{nX}\right)f_\sigma + 2\frac{XU'}{U^2}\sigma f_{\sigma\sigma}$$

$$-2Xf_{\sigma\sigma}\sum_{n=0}^{\infty}f_{\zeta_n}\zeta_{nX} + 4\frac{X}{U}\sum_{n=0}^{\infty}f_{\sigma\zeta_n}\zeta_{nT} \tag{14}$$

$$h_{\sigma\sigma} + Prfh_\sigma = 4Pr\left[\frac{\sigma XU'}{2U^2}h_\sigma + \frac{X}{U}\sum_{n=0}^{\infty}h_{\zeta_n}\zeta_{nT} + \frac{X}{2}\left(f_\sigma\sum_{n=0}^{\infty}h_{\zeta_n}\zeta_{nX} - h_\sigma\sum_{n=0}^{\infty}f_{\zeta_n}\zeta_{nX}\right)\right] \tag{15}$$

$$s_{\sigma\sigma} + Prfs_\sigma + \frac{Pr}{2}(f_{\sigma\sigma})^2 = 4Pr\left[\frac{\sigma}{2}\frac{XU'}{U^2}s_\sigma + 2\frac{XU'}{U^2}s + \frac{X}{U}\sum_{n=0}^{\infty}s_{\zeta_n}\zeta_{nT} + \frac{X}{2}\left(f_\sigma\sum_{n=0}^{\infty}s_{\zeta_n}\zeta_{nX} - s_\sigma\sum_{n=0}^{\infty}f_{\zeta_n}\zeta_{nX}\right)\right] \tag{16}$$

Equations (15) and (16) are correct only if the quantity $C\nu_\infty$ is constant. For the case considered herein (constant θ_w), equation (4) shows that $C\nu_\infty$ is indeed constant. The boundary conditions (eqs. (9) and (10)), in terms of the definitions (12) and (13), are

$$f_\sigma(\infty,\zeta_n) = 2; \qquad f_\sigma(0,\zeta_n) = f(0,\zeta_n) = 0 \tag{17}$$

$$h(\infty,\zeta_n) = 0; \qquad h(0,\zeta_n) = 1 \tag{18}$$

$$s(\infty,\zeta_n) = 0; \qquad s(0,\zeta_n) = 0 \tag{19}$$

Since nearly quasi-steady flows are assumed here, no initial conditions need be specified.

Equations (14) to (16) can be made self-consistent (i.e., functions of σ and ζ_n, only) by defining

$$\zeta_0 \equiv \frac{XU'}{U^2}; \qquad \zeta_1 \equiv \frac{X^2U''}{U^3}; \qquad \zeta_2 \equiv \frac{X^3U'''}{U^4}; \quad \cdots \tag{20}$$

These definitions correspond to the quantities (11); and, since the ratio of diffusion time to the characteristic free-stream variation time

and, hence, the ζ_n given by (20) are assumed small relative to unity, the functions f, h, and s may be expanded as follows:

$$f(\sigma,\zeta_n) \equiv F(\sigma) + \zeta_0 f_0(\sigma) + \zeta_1 f_1(\sigma) + \ldots + \zeta_0^2 f_{00}(\sigma) + \ldots + \zeta_0 \zeta_1 f_{01}(\sigma) + \ldots$$

$$\tag{21}$$

$$h(\sigma,\zeta_n) \equiv H(\sigma) + \zeta_0 h_0(\sigma) + \zeta_1 h_1(\sigma) + \ldots + \zeta_0^2 h_{00}(\sigma) + \ldots + \zeta_0 \zeta_1 h_{01}(\sigma) + \ldots$$

$$\tag{22}$$

$$s(\sigma,\zeta_n) \equiv S(\sigma) + \zeta_0 s_0(\sigma) + \zeta_1 s_1(\sigma) + \ldots + \zeta_0^2 s_{00}(\sigma) + \ldots + \zeta_0 \zeta_1 s_{01}(\sigma) + \ldots$$

$$\tag{23}$$

A discussion of the magnitudes of the ζ_n is presented in reference 1. It is there pointed out that in practical situations the requirement of small ζ_n is commonly met; and, furthermore, the ζ_n generally form a diminishing sequence, provided that $U(T)$ is a differentiable function. The limitations for small ζ_n for various specific $U(T)$ are also discussed in reference 1.

Substituting equations (21) to (23) into equations (14) to (19) and collecting coefficients of the various powers and products of the ζ_n yield in part (up to order ζ_1)

$$F''' + FF'' = 0 \tag{24a}$$

$$f_0''' + Ff_0'' - 2F'f_0' + 3F''f_0 = -4(2 - F') + 2\sigma F''' \tag{24b}$$

$$f_1''' + Ff_1'' - 4F'f_1' + 5F''f_1 = 4f_0' \tag{24c}$$

$$\vdots$$

$$F'(\infty) = 2; \qquad F'(0) = F(0) = 0 \tag{25a}$$

$$f_n'(\infty) = f_n'(0) = f_n(0) = 0 \tag{25b}$$

$$H'' + PrFH' = 0 \tag{26a}$$

$$h_0'' + PrFh_0' - 2PrF'h_0 = PrH'(2\sigma - 3f_0) \tag{26b}$$

$$h_1'' + \text{PrF}h_1' - 4\text{PrF}'h_1 = \text{Pr}(4h_0 - 5H'f_1) \tag{26c}$$

$$\vdots$$

$$H(\infty) = 0; \qquad H(0) = 1 \tag{27a}$$

$$h_n(\infty) = h_n(0) = 0 \tag{27b}$$

$$S'' + \text{PrF}S' + \frac{\text{Pr}}{2}(F'')^2 = 0 \tag{28a}$$

$$s_0'' + \text{PrF}s_0' - 2\text{PrF}'s_0 = \text{Pr}(2\sigma S' + 8S - F''f_0'' - 3S'f_0) \tag{28b}$$

$$s_1'' + \text{PrF}s_1' - 4\text{PrF}'s_1 = \text{Pr}(4s_0 - F''f_1'' - 5S'f_1) \tag{28c}$$

$$\vdots$$

$$S(\infty) = S(0) = 0 \tag{29a}$$

$$s_n(\infty) = s_n(0) = 0 \tag{29b}$$

Equations (24a), (25a), (26a), (27a), (28a), and (29a) are the equations appropriate for steady flow, where, of course, F is the Blasius function, where H describes the temperature distribution for an isothermal plate if the dissipation is neglected, and where

$$S(\sigma) = R(\sigma) - R(0) H(\sigma) \tag{30}$$

The $R(\sigma)$ is the solution for an insulated plate, and $R(0)$ is the recovery factor. The functions F, H, and R are tabulated in numerous papers; for example, F and H can be found in reference 6, and R is given in reference 1. Since the cited equations represent steady flow, equations (21) to (23), accordingly, indicate that for small ζ_n the laminar compressible boundary layer on an isothermal flat plate is nearly quasi steady with respect to both the velocity and temperature distributions. Hence, the first-order deviations from the quasi-steady case will be determined by solving equations (24b), (24c), (26b), (26c), (28b), and (28c) with their associated boundary conditions.

Solutions of momentum equations. - Since the momentum equation was made independent of the energy equation by the transformation given by equation (5), the solutions of equations (24) and (25) are not altered by a change in the thermal boundary conditions. Therefore, the functions F, f_0, f_1, and their derivatives for the case of an isothermal plate considered herein are identical to those for an insulated plate

as treated in reference 1. The function F and its derivatives, as has been stated, are tabu-
lated for Pr = 0.72 in reference 6, and the functions f_0, f_1, and their derivatives were de-
termined for Pr = 0.72 by direct numerical integration in reference 1 and are presented
therein.

Solutions of energy equations. - The solution of equations (26a) and (27a) is known and,
as has been stated, is tabulated in reference 6. The function H is presented in table I(a)
and figure 2(a) of this report for completeness. The function S, presented in table I(b) and
figure 2(b), is determined from equation (30) using the known H and R, the latter being tab-
ulated for Pr = 0.72 in reference 1. The remaining energy equations and their associated
boundary conditions (eqs. (26b), (26c), and (27b), and (28b), (28c), and (29b)) are solved for
Pr = 0.72 by the numerical integration method described in detail in appendix C of reference 1.
An outline of the method is presented herein in appendix B. The functions h_0 and h_1 are
presented for Pr = 0.72 in table I(a) and figure 2(a), and s_0 and s_1 for Pr = 0.72 are
given in table I(b) and figure 2(b).

UNSTEADY BOUNDARY-LAYER CHARACTERISTICS

Velocity and Temperature Profiles

The velocity and temperature distributions can be obtained from

$$\frac{u}{U} = \frac{1}{2}\left[F'(\sigma) + \zeta_0 f_0'(\sigma) + \zeta_1 f_1'(\sigma) + \ldots \right]$$

$$\frac{\theta - \theta_\infty}{\theta_w - \theta_\infty} = H + \frac{U^2}{2c_p(\theta_w - \theta_\infty)}\, S + \zeta_0\left[h_0 + \frac{U^2}{2c_p(\theta_w - \theta_\infty)}\, s_0 \right] + \zeta_1\left[h_1 + \frac{U^2}{2c_p(\theta_w - \theta_\infty)}\, s_1 \right] \ldots$$

The relation between y and σ is

$$y = 2\sqrt{\frac{\nu_\infty x}{U}}\left[\sigma + \frac{\theta_w - \theta_\infty}{\theta_\infty}\int_0^\sigma H\, d\sigma + \frac{\Gamma - 1}{2}M_\infty^2\int_0^\sigma S\, d\sigma + \zeta_0\left(\frac{\theta_w - \theta_\infty}{\theta_\infty}\int_0^\sigma h_0 d\sigma + \frac{\Gamma - 1}{2}M_\infty^2\int_0^\sigma s_0 d\sigma\right) + \zeta_1\left(\frac{\theta_w - \theta_\infty}{\theta_\infty}\int_0^\sigma h_1 d\sigma + \frac{\Gamma - 1}{2}M_\infty^2\int_0^\sigma s_1 d\sigma\right) + \ldots \right]$$

The functions F and f_n are independent of the Mach number. Hence, the velocity profile is thickened (or thinned) because of compressibility. The specific effect can be determined from the preceding relation between y and σ and depends on the temperature ratio and the Mach number. The unsteady effects are associated with the terms containing the ζ_n. The functions H, h_0, h_1, S, s_0, and s_1 associated with the temperature profile are presented in figure 2.

Skin Friction

The local skin-friction coefficient may be written as

$$c_f \equiv \frac{\tau_w}{\frac{1}{2}\rho_\infty U^2} = \frac{1}{2}\sqrt{\frac{C\nu_\infty}{UX}}\left[F''(0) + \zeta_0 f_0''(0) + \zeta_1 f_1''(0) + \ldots\right]$$

where $\tau_w = \left[\mu(\partial u/\partial y)\right]_w$ is the wall shear stress. Substituting the values of $F''(0)$, $f_0''(0)$, and $f_1''(0)$ for $Pr = 0.72$ given in references 1 and 6 yields

$$c_f = 0.6641\sqrt{\frac{C\nu_\infty}{UX}}\left[1 + 2.555\,\zeta_0 - 1.414\,\zeta_1 + \ldots\right] \tag{31}$$

Equation (31) has the same form as its counterpart for an insulated surface as given in reference 1, but the skin friction does differ for the case of heat transfer. The effect of heat transfer is accounted for by the constant C (see eq. (3)). From equation (4) it can be seen that C will be altered, because θ_w is the isothermal value specified herein rather than the adiabatic value used in reference 1.

The leading term on the right of equation (31) is the quasi-steady value of the coefficient. As would be expected, positive acceleration leads to larger values of skin friction than the quasi-steady value.

Displacement Thickness

The displacement thickness δ^* is defined as

$$\delta^* \equiv \int_0^\infty \left(1 - \frac{\rho}{\rho_\infty}\frac{u}{U}\right)dy$$

or, by use of equations (2), (5), (6), and (12),

$$\delta^* = \sqrt{\frac{XC\nu_\infty}{U}} \int_0^\infty \left(2\,\frac{\theta}{\theta_\infty} - f_\sigma\right) d\sigma$$

Introducing equations (7) and (13) gives

$$\delta^* = \sqrt{\frac{XC\nu_\infty}{U}} \int_0^\infty \left[2 + \frac{2(\theta_W - \theta_\infty)}{\theta_\infty} h + (\gamma - 1)M_\infty^2 s - f_\sigma\right] d\sigma$$

or, using equations (21) to (23),

$$\delta^* = \sqrt{\frac{XC\nu_\infty}{U}} \left\{ \lim_{\sigma\to\infty}(2\sigma - F) + (\gamma-1)M_\infty^2\int_0^\infty s\,d\sigma + \frac{2(\theta_W - \theta_\infty)}{\theta_\infty}\int_0^\infty H\,d\sigma + \zeta_0\left[-f_0(\infty) + (\gamma-1)M_\infty^2\int_0^\infty s_0 d\sigma + \frac{2(\theta_W - \theta_\infty)}{\theta_\infty}\int_0^\infty h_0 d\sigma + \ldots\right] + \zeta_1\left[-f_1(\infty) + (\gamma-1)M_\infty^2\int_0^\infty s_1 d\sigma + \frac{2(\theta_W - \theta_\infty)}{\theta_\infty}\int_0^\infty h_1 d\sigma + \ldots\right] \right\}$$

Using the fact (ref. 1) that $\lim\limits_{\sigma\to\infty}(F - 2\sigma) = -1.721$ and the information given in table I,

$$\delta^* = 1.721\sqrt{\frac{XC\nu_\infty}{U}}\left\{1 + 0.1873(\gamma-1)M_\infty^2 + 1.1283\,\frac{\theta_W - \theta_\infty}{\theta_\infty} - 0.5919\,\zeta_0\left[1 + 0.4359(\gamma-1)M_\infty^2 - 0.08688\,\frac{\theta_W - \theta_\infty}{\theta_\infty}\right] + 0.5944\,\zeta_1\left[1 + 0.2590(\gamma-1)M_\infty^2 + 0.5295\,\frac{\theta_W - \theta_\infty}{\theta_\infty}\right] + \ldots\right\} \tag{32}$$

The first three terms on the right correspond to the compressible quasi-steady result, as can be verified for a given Mach number and temperature in reference 6. The effects of heat transfer not only affect the quasi-steady results through C and $(\theta_W - \theta_\infty)/\theta_\infty$, but also are of importance in the deviations from the quasi steady. For example, if $\theta_W < \theta_\infty$, a positive acceleration will lead to a thinner boundary layer than the quasi steady, as was the case also for an insulated surface. However, if $\theta_W > \theta_\infty$, the boundary layer will depend on the magnitude of the Mach number as well as the temperature difference.

Local Rate of Heat Transfer

The local rate of heat transfer is given by

$$q \equiv -k\left(\frac{\partial \theta}{\partial y}\right)_W$$

Using the definition of the Prandtl number and equations (2), (3), (5), (7), and (13) in the above expression yields

$$q = -\frac{c_p}{2Pr}(\theta_W - \theta_\infty)\sqrt{\frac{U\mu_\infty\rho_\infty C}{X}}\left[h_\sigma + \frac{U^2}{2c_p(\theta_W - \theta_\infty)}s_\sigma\right]_W$$

or, using equations (22) and (23),

$$q = -\frac{c_p}{2Pr}(\theta_W - \theta_\infty)\sqrt{\frac{U\mu_\infty\rho_\infty C}{X}}\left\{H'(0) + \frac{U^2}{2c_p(\theta_W - \theta_\infty)}s'(0) + \zeta_0\left[h'_0(0) + \frac{U^2}{2c_p(\theta_W - \theta_\infty)}s'_0(0) + \ldots\right] + \zeta_1\left[h'_1(0) + \frac{U^2}{2c_p(\theta_W - \theta_\infty)}s'_1(0) + \ldots\right]\right\}$$

Substituting the numerical values from table I yields for $Pr = 0.72$

$$q = 0.4106\, c_p(\theta_W - \theta_\infty)\sqrt{\frac{U\mu_\infty\rho_\infty C}{X}}\left\{1 - 0.4240(\gamma - 1)M_\infty^2\frac{\theta_\infty}{\theta_W - \theta_\infty} - 0.06923\,\zeta_0\left[1 + 0.2746(\gamma - 1)M_\infty^2\frac{\theta_\infty}{\theta_W - \theta_\infty}\right] - 0.4232\,\zeta_1\left[1 - 0.5504(\gamma - 1)M_\infty^2\frac{\theta_\infty}{\theta_W - \theta_\infty}\right] + \ldots\right\}$$

$$(33)$$

The compressible quasi-steady heat-transfer rate is given by the first two terms on the right side of equation (33), as can be seen by comparing with equation (21) of reference 6.

The deviations from the quasi-steady results depend again on the magnitudes of the temperature difference and Mach number. For example, for positive acceleration the heat-transfer rate from the plate is decreased if $\theta_W > \theta_\infty$, but if $\theta_W < \theta_\infty$ it might either be increased or decreased.

Plate Oscillating About a Steady Velocity

As an example of the foregoing analysis, suppose that the plate os-
cillates about a steady velocity as

$$U = u_0(1 + \varepsilon \sin \omega t) \tag{34}$$

where the amplitude of the velocity fluctuations ε is to be small rel-
ative to unity. Substituting equation (34) into equations (31) and (33)
yields to order ε

$$c_f = c_{f_0}\left[1 + \varepsilon C_1 \sin(\omega t + \varphi_1)\right] \tag{35}$$

and

$$q = q_0\left[1 + \varepsilon C_2 \sin(\omega t - \varphi_2)\right] \tag{36}$$

where c_{f_0} and q_0 are the steady (corresponding to flight velocity
u_0) local skin-friction coefficient and heat-transfer rate, respec-
tively, and where

$$C_1 = 1.5 + 3.590\left(\frac{x\omega}{u_0}\right)^2 + \mathcal{O}\left[\left(\frac{x\omega}{u_0}\right)^4\right] \tag{37}$$

$$\varphi_1 = \tan^{-1} 1.703\left(\frac{x\omega}{u_0}\right)\left\{1 + \mathcal{O}\left[\left(\frac{x\omega}{u_0}\right)^2\right]\right\} \tag{38}$$

for $\beta \neq \dfrac{1}{2.120}$,

$$C_2 = \left|\frac{1 - 2.120\beta}{2(1 - 0.424\beta)}\left\{1 + \frac{0.8560 - 2.2550\beta + 0.9883\beta^2}{(1 - 2.120\beta)^2}\left(\frac{x\omega}{u_0}\right)^2 + \mathcal{O}\left[\left(\frac{x\omega}{u_0}\right)^4\right]\right\}\right| \tag{39a}$$

$$\varphi_2 = \tan^{-1}\left\{\frac{0.1385(1 + 0.2746\beta)\left(\frac{x\omega}{u_0}\right)}{1 - 2.120\beta}\left(1 + \mathcal{O}\left[\left(\frac{x\omega}{u_0}\right)^2\right]\right)\right\} \tag{40a}$$

and, for $\beta = \dfrac{1}{2.120}$,

$$C_2 = 0.09775\frac{x\omega}{u_0}\left\{1 + \mathcal{O}\left[\left(\frac{x\omega}{u_0}\right)^2\right]\right\} \tag{39b}$$

$$\varphi_2 = \tan^{-1} 0.2496 \frac{u_0}{x_{\mathrm{D}}} \left\{ 1 + \beta \left[\left(\frac{x_{\mathrm{D}}}{u_0} \right)^2 \right] \right\} \tag{40b}$$

where

$$\beta = \frac{(\gamma - 1)M_0^2 \theta_\infty}{\theta_w - \theta_\infty} \tag{41}$$

The quadrants of the angles φ_1 and φ_2 can be determined from the respective signs of the numerator and denominator of the defining equations.

It is significant to note from equations (34) to (36) that the maxima of skin friction and heat transfer are not in phase with the maxima of the plate velocity; and, furthermore, the amplitude of the fluctuations of these quantities depends on the frequency, as was also found in reference 2.

Note that equations (35) and (36) give the deviations from the steady (or mean) conditions rather than from the quasi steady as was the case in the discussion of the general analysis. The functions C_1 and C_2 (which define the maximum deviations from the steady) and the phase angles φ_1 and φ_2 are presented in figure 3. It can be seen from the definition of φ_1 and figure 3(a) that for permissible values of $\frac{x_{\mathrm{D}}}{u_0}$ the maxima in skin friction will always lead the plate velocity by angles not exceeding about 45°. The phase relations between the heat-transfer rate and the plate velocity depend essentially on the Mach number, ratio of plate to stream temperature, and frequency. For Mach numbers near zero, φ_2 becomes small, and the maxima of heat transfer and plate velocity are nearly in phase in accord with the discussion in reference 2.

From figure 3 it can be seen that the unsteady effects can be significant. It should be noted from equations (36) and (39) that C_2 becomes infinite when the steady heat transfer approaches zero. The actual heat-transfer rate given by equation (36) is, however, finite. The function C_2 remains almost constant with $\frac{x_{\mathrm{D}}}{u_0}$ (see fig. 3(b)), so that the maximum amplitude of the heat-transfer fluctuations is essentially the quasi-steady value.

CONCLUDING REMARKS

The laminar compressible boundary-layer flow and heat transfer over an isothermal semi-infinite flat plate moving with a time-dependent velocity has been analyzed. The first-order deviations of the velocity and temperature profiles, skin-friction coefficient, displacement thickness, and local heat-transfer rate from the quasi steady have been computed; the associated universal functions are presented in tabular form for $Pr = 0.72$. Relative to quasi-steady flow, positive acceleration results in larger skin friction, thinner boundary layers if the wall temperature is larger than the free-stream temperature, and either thicker or thinner boundary layers (depending on the Mach number) if the surface is at a lower temperature than the stream. Positive acceleration results in lower heat-transfer rates from the plate if the surface temperature is greater than the free stream, whereas with lower surface temperatures the heat-transfer rate would be increased or decreased depending on the magnitudes of the temperature difference and the Mach number. Hence, the boundary-layer characteristics for an isothermal surface can be considerably different from those for an insulated surface.

Consideration of the particular case of a plate oscillating about a steady velocity showed that the boundary-layer characteristics can be appreciably altered by the unsteady effects. Furthermore, the skin friction and local heat-transfer rates were found to be out of phase with the plate velocity for permissible values of the frequency parameter. The maxima of skin friction lead the plate velocity by amounts not greater than about $45°$. For steady Mach numbers near zero, the heat transfer is almost in phase with the plate velocity. At higher speeds the heat-transfer phase angle depends significantly on the steady Mach number and ratio of wall to free-stream temperature in addition to the frequency.

Lewis Flight Propulsion Laboratory
        National Advisory Committee for Aeronautics
              Cleveland, Ohio, August 10, 1955

APPENDIX A

SYMBOLS

A   acceleration

C   constant defined by eq. (4)

C_1, C_2 constants defined by eqs. (37) and (39), respectively

c_f local skin-friction coefficient

c_p specific heat at constant pressure

F   related to stream function for flat plate in steady flow

f, f_i functions related to stream function for unsteady flat-plate
            flow, $i = 0, 1, 2, \ldots$

H   temperature function related to steady flat-plate flow

h, h_i functions related to temperature for unsteady flat-plate flow,
            $i = 0, 1, 2, \ldots$

k   thermal conductivity coefficient.

M   Mach number

Pr   Prandtl number

q   local heat-transfer rate

R   function related to temperature profile for insulated flat plate
            in steady flow

S   function related to temperature for steady flat-plate flow

s, s_i functions related to temperature for unsteady flat-plate flow,
            $i = 0, 1, 2, \ldots$

$T, t, \bar{t}$ time

U   stream velocity in x-direction

$u, \bar{u}$ velocity in X- and x-directions, respectively

$v, \bar{v}$ velocity in Y- and y-directions, respectively

$X, x, \bar{x}$ coordinate along surface

$Y, y, \bar{y}$ coordinate normal to surface

β constant defined by eq. (41)

γ ratio of specific heats

δ^* displacement thickness

ε amplitude of velocity fluctuations

ζ_n dimensionless parameter, $n = 0, 1, 2, \ldots$ (eq. (20))

Θ dimensionless temperature difference

θ temperature

μ absolute viscosity coefficient

ν_∞ kinematic viscosity coefficient outside boundary layer

ρ density

σ dimensionless coordinate, $\dfrac{Y}{2}\sqrt{\dfrac{U}{C\nu_\infty X}}$

φ_1, φ_2 phase angles defined by eqs. (38) and (40), respectively

ψ stream function

ω frequency of velocity fluctuations

Subscripts:

w   evaluation at wall $(y = 0)$

0   evaluation at a steady condition

∞ evaluation in stream $(y \to \infty)$

     Subscript notation for partial differentiation is used when convenient. Primes denote ordinary differentiation.

APPENDIX B

INTEGRATION METHOD

The second-order differential equations for the temperature functions (eqs. (26b), (26c), (28b), and (28c)) and their associated boundary conditions (eqs. (27a), (27b), (29a), and (29b)) constitute a two-point boundary-value problem. The difficulty presented by the fact that the boundary conditions are given at two points ($\sigma = 0, \infty$) is overcome by splitting the original two-point problem into two single-point problems. To this end, each function h_0, h_1, s_0, and s_1 is written as the sum of two functions; for example, for h_0, as

$$h_0 = - \left[\lim_{\sigma \to \infty} \frac{h_0^{(2)}(\sigma)}{h_0^{(1)}(\sigma)} \right] h_0^{(1)}(\sigma) + h_0^{(2)}(\sigma)$$

where the $h_0^{(1)}(\sigma)$ and $h_0^{(2)}(\sigma)$ are solutions of single-point problems. The $h_0^{(1)}$ satisfies the homogeneous equation with the specified initial condition plus an arbitrary initial condition $\left(h_0^{(1)} \right)'(0) = 1$ replacing the boundary condition at infinity, and the $h_0^{(2)}(\sigma)$ satisfies the non-homogeneous equation and homogeneous initial conditions on the function and its first derivative.

The scale of the variable σ is then divided into equal intervals. Starting from the initial values of each part of each function - for example, $h_0^{(1)}(\sigma)$ and $h_0^{(2)}(\sigma)$ - the values at successive points near $\sigma = 0$ can be obtained by expanding the unknown function in a Maclaurin series. Thus, the function and its derivatives are known at a successive number of points near $\sigma = 0$. A polynomial (for the highest derivative) can then be matched to the known values and to the unknown value at the next point. The degree of the polynomial and size of the interval depend on the accuracy required. In this regard, it can be stated that the solutions of the energy equations are more easily obtained than those of the momentum equations, since a second-degree polynomial is matched at three successive points for the temperature functions, whereas a fifth-degree polynomial was matched at six points in the solution of the momentum equations (see ref. 1). This simplification is considered warranted, because the energy equations are of lower order than the momentum equations. However, because the curvatures of the s_0 and s_1

functions were relatively greater than the h_0 and h_1 functions (see fig. 2), it was decided to check the accuracy of the three-point method described herein. Accordingly, s_0 and its derivatives were obtained by five-point integration formulas, and those results for s_0 differed by at most one in the fourth decimal place and by two in the fourth place for s_0' from those presented herein.

The polynomial is then integrated to yield the successively lower-order derivatives at the unknown point in terms of the known and unknown values of the highest derivative. The condition that the function and all its derivatives must satisfy the differential equation at the unknown point serves to determine the highest-order derivative and, hence, the function at that point. Thus, given the function at a successive number of points, the solution can be extended to the next point. This procedure is then continued over the entire range of σ.

REFERENCES

1. Moore, Franklin K.: Unsteady Laminar Boundary-Layer Flow. NACA TN 2471, 1951.

2. Lighthill, M. J.: The Response of Laminar Skin Friction and Heat Transfer to Fluctuations in the Stream Velocity. Proc. Roy. Soc. (London), ser. A, vol. 224, June 1954, pp. 1-23.

3. Chapman, Dean R., and Rubesin, Morris W.: Temperature and Velocity Profiles in the Compressible Laminar Boundary Layer with Arbitrary Distribution of Surface Temperature. Jour. Aero. Sci., vol. 16, no. 9, Sept. 1949, pp. 547-565.

4. Howarth, L.: Concerning the Effect of Compressibility on Laminar Boundary Layers and Their Separation. Proc. Roy. Soc. (London), ser. A, vol. 194, no. 1036, July 28, 1948, pp. 16-42.

5. Illingworth, C. R.: Unsteady Laminar Flow of Gas Near an Infinite Flat Plate. Proc. Cambridge Phil. Soc., vol. 46, 1950, pp. 603-613.

6. Low, George M.: The Compressible Laminar Boundary Layer with Fluid Injection. NACA TN 3404, 1955.

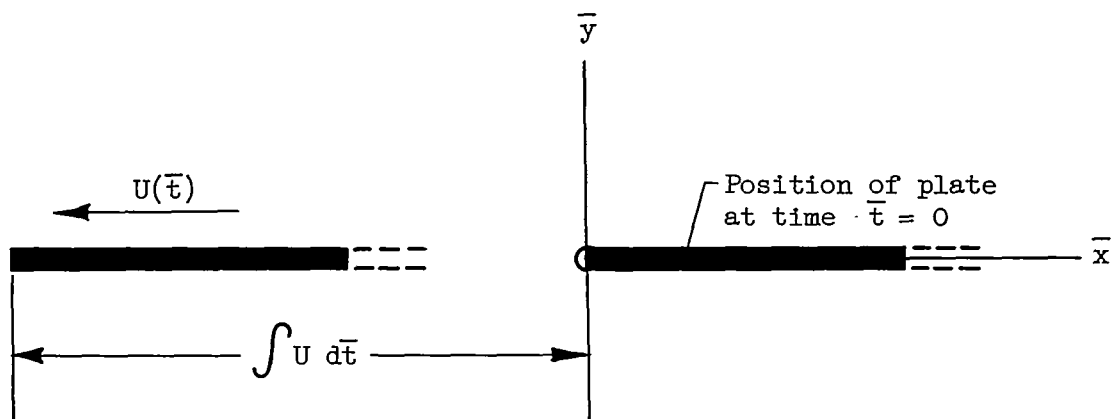## TABLE I. - FUNCTIONS ASSOCIATED WITH TEMPERATURE PROFILE

(a) Functions h.

σ	H	H'	h_0	h_0'	h_1	h_1'
0	1.0	-0.5912	0.00000	0.04093	0.00000	0.25019
.1	.9409	-.5911	.00397	.03737	.02503	.25039
.2	.8818	-.5905	.00732	.02915	.05004	.24939
.3	.8228	-.5887	.00976	.01934	.07430	.24500
.4	.7641	-.5853	.01122	.01014	.09887	.23539
.5	.7058	-.5796	.01186	.00300	.12167	.21932
.6	.6483	-.5713	.01192	-.00135	.14251	.19631
.7	.5917	-.5599	.01170	-.00275	.16070	.16659
.8	.5364	-.5452	.01146	-.00152	.17562	.13108
.9	.4827	-.5269	.01145	.00169	.18677	.09127
1.0	.4311	-.5050	.01183	.00603	.19379	.04908
1.1	.3819	-.4797	.01266	.01057	.19657	.00660
1.2	.3353	-.4512	.01391	.01448	.19518	-.03405
1.3	.2917	-.4199	.01551	.01708	.18989	-.07092
1.4	.2513	-.3865	.01727	.01796	.18118	-.10244
1.5	.2144	-.3516	.01904	.01697	.16963	-.12749
1.6	.1811	-.3161	.02061	.01423	.15591	-.14548
1.7	.1512	-.2805	.02184	.01002	.14076	-.15633
1.8	.1249	-.2458	.02258	.00479	.12487	-.16042
1.9	.1020	-.2125	.02278	-.00082	.10887	-.15850
2.0	.0824	-.1812	.02242	-.00631	.09333	-.15159
2.1	.0657	-.1524	.02153	-.01122	.07868	-.14086
2.2	.0518	-.1264	.02020	-.01524	.06523	-.12749
2.3	.0403	-.1034	.01851	-.01816	.05321	-.11264
2.4	.0310	-.0834	.01660	-.01992	.04272	-.09730
2.5	.0236	-.0663	.01457	-.02057	.03374	-.08227
2.6	.0176	-.0520	.01252	-.02025	.02623	-.06817
2.7	.0131	-.0401	.01055	-.01919	.02006	-.05538
2.8	.0095	-.0306	.00870	-.01760	.01510	-.04415
2.9	.0069	-.0230	.00703	-.01564	.01117	-.03461
3.0	.0049	-.0170	.00557	-.01351	.00812	-.02665
3.1	.0035	-.0124	.00432	-.01136	.00579	-.02019
3.2	.0024	-.0089	.00329	-.00933	.00404	-.01507
3.3	.0016	-.0063	.00246	-.00748	.00274	-.01107
3.4	.0011	-.0044	.00179	-.00588	.00180	-.00805
3.5	.0007	-.0030	.00127	-.00452	.00110	-.00581
3.6	.0005	-.0021	.00087	-.00342	.00061	-.00418
3.7	.0003	-.0013	.00057	-.00254	.00026	-.00303
3.8	.0002	-.0009	.00036	-.00184	.00000	-.00221
3.9	.0001	-.0006	.00020	-.00134	-.00019	-.00168
4.0	.0001	-.0004	.00009	-.00096	-.00035	-.00136
4.1	.0000	-.0002	.00001	-.00068	-.00048	-.00116

$$\int_0^\infty H\,d\sigma = 0.9692 \qquad \int_0^\infty h_0\,d\sigma = 0.04425 \qquad \int_0^\infty h_1\,d\sigma = 0.3158$$

TABLE I. - Concluded. FUNCTIONS ASSOCIATED WITH TEMPERATURE PROFILE

(b) Functions s.

σ	S	S'	s_0	s_0'	s_1	s_1'
0	0.00000	0.50134	0.00000	0.02248	0.00000	-0.27540
.1	.04694	.43775	-.01217	-.24852	-.01863	-.09863
.2	.08754	.37395	-.04648	-.42273	-.02027	.06196
.3	.12176	.30988	-.09399	-.51508	-.00719	.19431
.4	.14953	.24593	-.14724	-.53969	.01741	.29163
.5	.17099	.18287	-.20013	-.51025	.04987	.35127
.6	.18614	.12174	-.24794	-.44003	.08643	.37400
.7	.19540	.06368	-.28721	-.34181	.12356	.36311
.8	.19905	.01006	-.31577	-.22761	.15812	.32417
.9	.19766	-.03789	-.33257	-.10845	.18770	.26433
1.0	.19174	-.07898	-.33761	.00616	.21053	.19060
1.1	.18205	-.11227	-.33176	.10850	.22561	.11051
1.2	.16953	-.13732	-.31651	.19305	.23264	.03094
1.3	.15491	-.15411	-.29384	.25662	.23200	-.04225
1.4	.13905	-.16293	-.26591	.29822	.22455	-.10467
1.5	.12261	-.16462	-.23490	.31885	.21152	-.15350
1.6	.10625	-.16019	-.20276	.32099	.19434	-.18760
1.7	.09070	-.15159	-.17119	.30819	.17447	-.20734
1.8	.07615	-.13899	-.14149	.28445	.15329	-.21424
1.9	.06297	-.12436	-.11454	.25375	.13199	-.21036
2.0	.05125	-.10883	-.09085	.21959	.11150	-.19835
2.1	.04119	-.09328	-.07065	.18486	.09250	-.18082
2.2	.03259	-.07843	-.05384	.15171	.07544	-.16012
2.3	.02548	-.06475	-.04021	.12155	.06051	-.13820
2.4	.01961	-.05254	-.02941	.09517	.04777	-.11657
2.5	.01485	-.04196	-.02104	.07283	.03714	-.09628
2.6	.01121	-.03295	-.01471	.05449	.02844	-.07797
2.7	.00822	-.02558	-.01003	.03985	.02146	-.06202
2.8	.00605	-.01945	-.00665	.02842	.01597	-.04848
2.9	.00431	-.01460	-.00427	.01979	.01169	-.03723
3.0	.00305	-.01082	-.00263	.01339	.00844	-.02814
3.1	.00207	-.00790	-.00152	.00878	.00601	-.02093
3.2	.00143	-.00570	-.00082	.00555	.00421	-.01533
3.3	.00098	-.00405	-.00039	.00336	.00289	-.01107
3.4	.00063	-.00283	-.00014	.00193	.00196	-.00787
3.5	.00042	-.00198	.00002	.00101	.00130	-.00551
3.6	.00021	-.00129	.00008	.00046	.00085	-.00381
3.7	.00013	-.00096	.00011	.00013	.00053	-.00259
3.8	.00004	-.00060	.00012	-.00004	.00031	-.00176
3.9	.00002	-.00037	.00010	-.00012	.00017	-.00117
4.0	.00005	-.00023	.00009	-.00015	.00008	-.00077
4.1	0	-.00019	.00008	-.00015	.00002	-.00051

$$\int_0^\infty S\, d\sigma = 0.2879 \qquad \int_0^\infty s_0\, d\sigma = -0.4440 \qquad \int_0^\infty s_1\, d\sigma = 0.3095$$

3743

3743

(a) Coordinates fixed in fluid at rest.
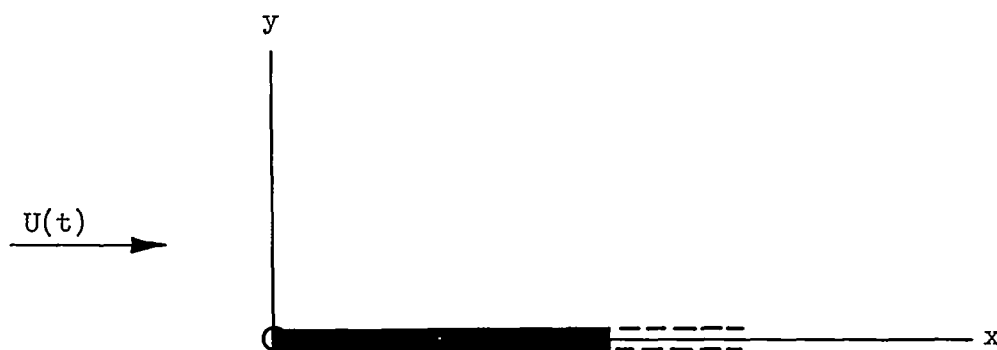
(b) Coordinates fixed in plate.

Figure 1. - Coordinate systems used in analysis.
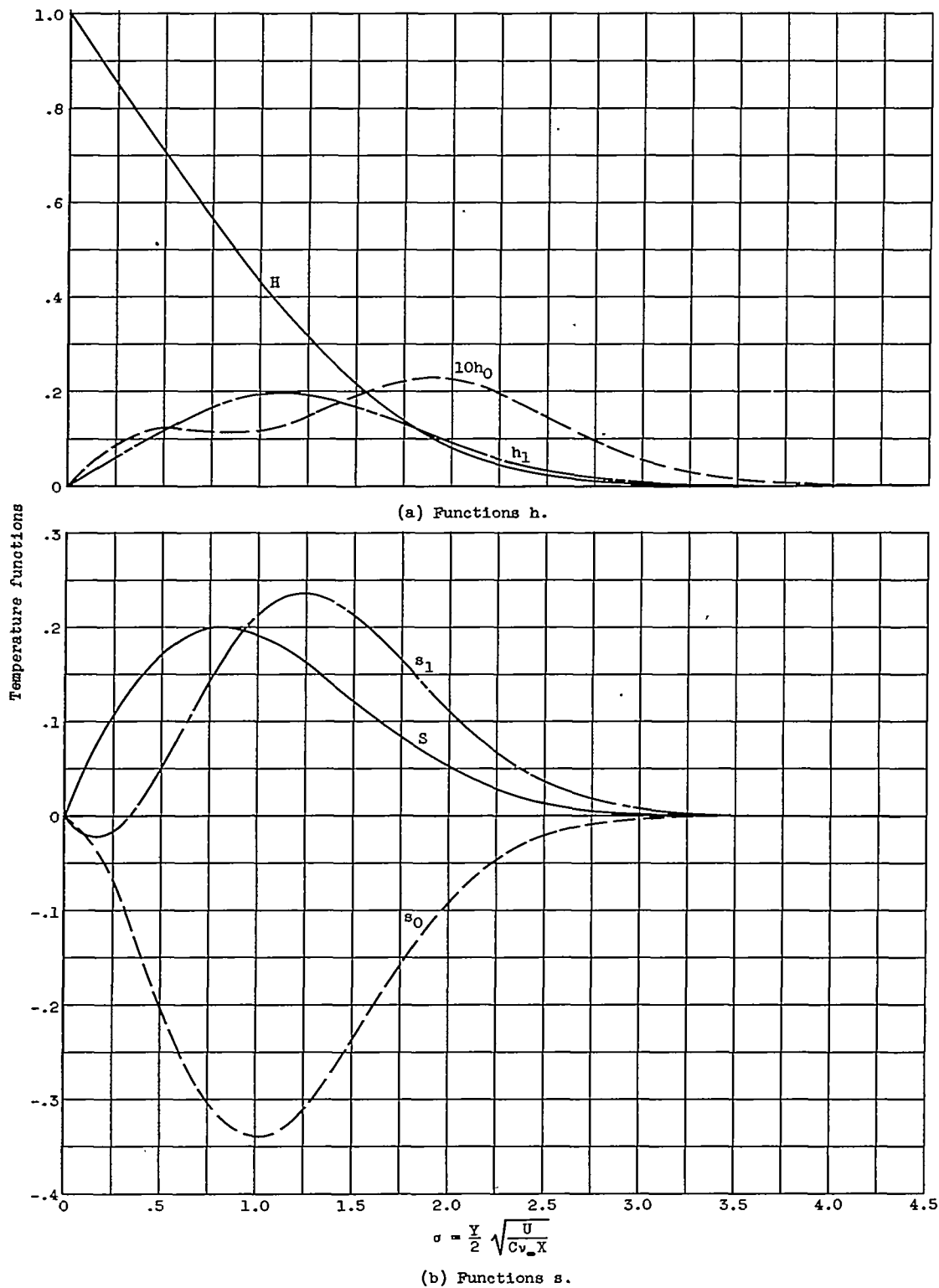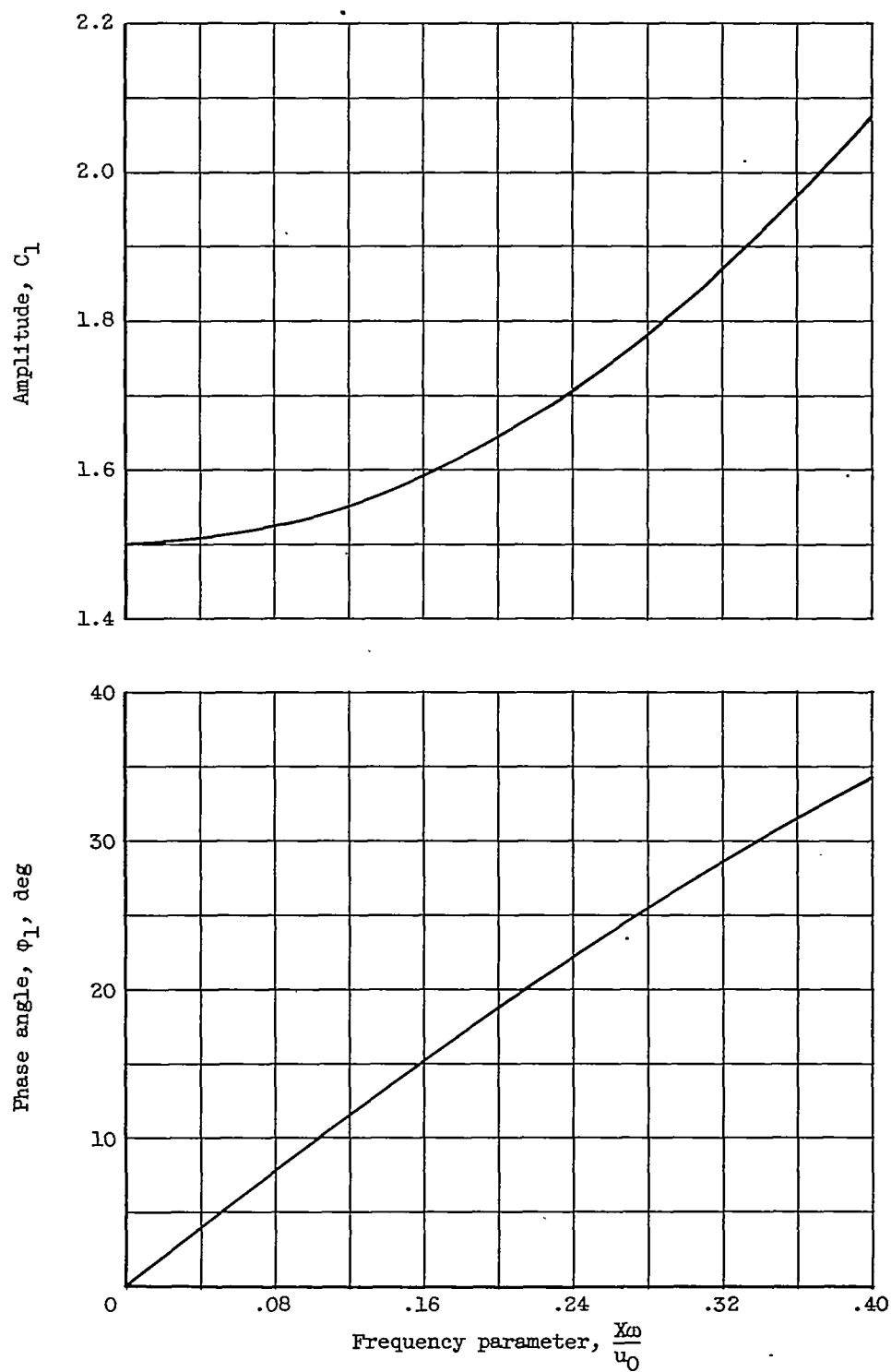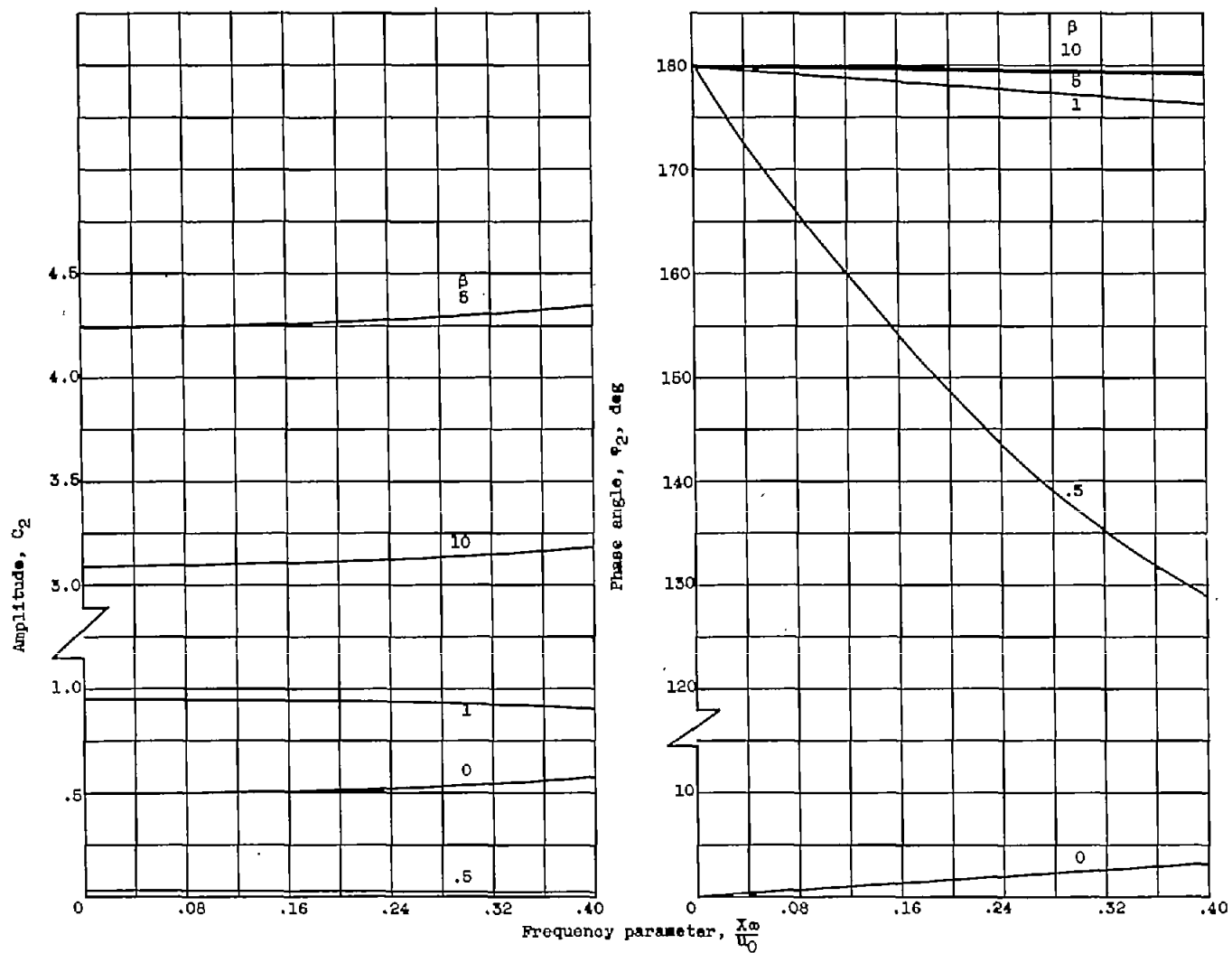
(a) Functions h.

(b) Functions s.

Figure 2. - Functions associated with temperature profile.

(a) Skin-friction fluctuations.

Figure 3. - Amplitudes and phase angles as functions of fre-
quency parameter for plate oscillating about a steady
velocity.

(b) Heat-transfer fluctuations.

Figure 3. - Concluded. Amplitudes and phase angles as functions of frequency parameter for plate oscillating about a steady velocity.